

Article

Sixteen Years of Agricultural Drought Assessment of the BioBío Region in Chile Using a 250 m Resolution Vegetation Condition Index (VCI)

Francisco Zambrano ^{1,*}, Mario Lillo-Saavedra ^{1,2,*}, Koen Verbist ^{3,4} and Octavio Lagos ^{1,2}

¹ Department of Water Resources, Universidad de Concepción, Chillán 3801061, Chile; octaviolagos@udec.cl

² Water Research Center for Agriculture and Mining (CRHIAM) (CONICYT-FONDAP-15130015), Concepción 4070411, Chile

³ UNESCO-IHP, Hydrological Systems and Global Change Section, Santiago 7511019, Chile; k.verbist@unesco.org

⁴ International Centre for Eremology, Department of Soil Management, Ghent University, Ghent B-9000 Gent, Belgium

* Correspondence: frzambra@gmail.com (F.Z.); malillo@udec.cl (M.L.-S.); Tel.: +56-42-220-8807 (M.L.-S.)

† These authors contributed equally to this work.

Academic Editors: Anton Vrieling, Clement Atzberger and Prasad Thenkabail

Received: 7 March 2016; Accepted: 12 June 2016; Published: 22 June 2016

Abstract: Drought is one of the most complex natural hazards because of its slow onset and long-term impact; it has the potential to negatively affect many people. There are several advantages to using remote sensing to monitor drought, especially in developing countries with limited historical meteorological records and a low weather station density. In the present study, we assessed agricultural drought in the croplands of the BioBío Region in Chile. The vegetation condition index (VCI) allows identifying the temporal and spatial variations of vegetation conditions associated with stress because of rainfall deficit. The VCI was derived at a 250 m spatial resolution for the 2000–2015 period with the Moderate Resolution Imaging Spectroradiometer (MODIS) MOD13Q1 product. We evaluated VCI for cropland areas using the land cover MCD12Q1 version 5.1 product and compared it to the in situ Standardized Precipitation Index (SPI) for six-time scales (1–6 months) from 26 weather stations. Results showed that the 3-month SPI (SPI-3), calculated for the modified growing season (November–April) instead of the regular growing season (September–April), has the best Pearson correlation with VCI values with an overall correlation of 0.63 and between 0.40 and 0.78 for the administrative units. These results show a very short-term vegetation response to rainfall deficit in September, which is reflected in the vegetation in November, and also explains to a large degree the variation in vegetation stress. It is shown that for the last 16 years in the BioBío Region we could identify the 2007/2008, 2008/2009, and 2014/2015 seasons as the three most important drought events; this is reflected in both the overall regional and administrative unit analyses. These results concur with drought emergencies declared by the regional government. Future studies are needed to associate the remote sensing values observed at high resolution (250 m) with the measured crop yield to identify more detailed individual crop responses.

Keywords: drought; MODIS; VCI; SPI; agriculture

1. Introduction

Drought is considered one of the most complex natural hazards because of its slow onset and long-term impact; it has the potential to negatively affect many people. Drought is caused by various

environmental factors that mainly changes the pattern and amount of rainfall. This situation is expected to intensify over time because of climate change [1]. The fifth report from the Intergovernmental Panel on Climate Change (IPCC) [2] projects an increase in global temperature and indicates that rainfall in south-central Chile will decrease. This will likely increase both drought frequency and intensity.

According to Wilhite and Glantz [3], drought can be classified into four categories: (1) Meteorological drought; (2) Hydrological drought; (3) Agricultural drought; and (4) Socio-economic drought. To monitor drought, many different indices were developed and applied to research areas, such as meteorology, hydrology, agriculture, and water resource management. Currently, there are more than 100 drought indices [4,5]. Among the most popular drought indices is the multiscalar Standardized Precipitation Index (SPI) [6], which is used to characterize meteorological drought. The SPI is estimated by frequency analysis of rainfall records; this requires a long-term record of precipitation data, preferably more than 30 years, to select an appropriate probability distribution [7]. The Standardized Precipitation Evapotranspiration Index (SPEI) is a more recent drought index developed by Vicente-Serrano *et al.* [8], which not only includes precipitation but also the effect of temperature. Another important meteorological drought index was developed by Palmer [9] with temperature and precipitation data to estimate moisture supply and demand in a two-layer soil model known as the Palmer Drought Severity Index (PDSI). However, as noted by Alley [10], this index has some limitations, such as the use of arbitrary rules to quantify it and limited methodology to standardize it. Using temperature and evapotranspiration (ET) data, Palmer [11] developed a crop moisture index (CMI), which was one of the first agricultural drought index. There are also hydrological drought indices, such as the surface water supply index (SWSI) [12] and standardized streamflow index (SSI) [13]. However, most of the aforementioned indices depend on the availability of temporal and spatial field data, thus complicating their implementation in data-scarce developing countries where historical record availability is limited and meteorological station density is insufficient. This situation does not allow adequate spatial mapping of the index that needs to be generated [14]. Furthermore, using discrete, point-based meteorological measurements collected at weather station locations has resulted in a restricted level of spatial precision for monitoring drought patterns [15]. Remote sensing, therefore, offers significant advantages for monitoring agricultural drought at the regional and local levels by allowing both spatial and temporal evaluations.

Remote sensing vegetation indices (VI) have been widely used to assess vegetation and drought conditions [16–23]. The vegetation health index (VHI) [19,24], temperature condition index (TCI) [19], and vegetation condition index (VCI) [25] are among the main drought indices based on remote sensing; they have been successfully applied in numerous case studies under many different environmental conditions around the globe [16,26–30]. There are drought indices based on the spatial feature of land surface temperature (T_s) and the normalized difference vegetation index (NDVI), as well as the vegetation temperature dryness index (TVDI) suggested by Sandholt *et al.* [31] and the vegetation temperature condition index (VTCI) developed by Wang *et al.* [32], which are time-dependent and usually region specific. All of these indices use NDVI as input, which is the most widely used index to monitor vegetation quantity, quality, and development. The indices based on NDVI are more useful during the plant growing seasons [33,34]. Given the physical complexity of drought, there is an ongoing development and improvement of remote sensing drought indices. Zhang *et al.* [35] used VCI to construct the time-integrated vegetation condition index (TIVCI), which considers the time lag effect on NDVI from climate factors; however, the time-lag effect of NDVI on meteorological data when monitoring drought requires more attention [35]. Du *et al.* [36] integrated multi-source remote sensing data with a moderate resolution imaging spectroradiometer (MODIS), and the tropical rainfall measuring mission (TRMM) explained the synthesized drought index (SDI), which is defined as a principal component of VCI, TCI and precipitation condition index (PCI). One limitation of this index occurs at a temporal scale that is shorter than a 1 month [36]. Meanwhile, Mu *et al.* [37] introduced the drought severity index (DSI) to monitor and detect drought on a global scale with a 1km spatial resolution

and 8-day, monthly, and yearly frequencies; this new index integrates satellite ET and NDVI. Recently, Enenkel *et al.* [38] develop the Enhanced Combined Drought Index (ECDI) which link rainfall, soil moisture, land surface temperature and vegetation status.

The VCI [39] was one of the first remote sensing drought indices widely used to monitor agricultural drought [16–18,36]; it is derived from NDVI, is easily calculated, and accessible for different spatial and temporal resolutions. The VCI concept was originally designed to extract the weather component from NDVI values [39], considering vegetative variations by climate factors rather than seasonality. Kogan [24] developed the TCI and then combined both VCI and TCI in the VHI drought index [19,24] to increase the accuracy of drought monitoring and explain the contribution of temperature in drought analysis, which also provided useful information for monitoring vegetation stress caused by soil saturation. In the present study, VCI was selected for its multiple advantages and mainly because it not only reflects spatial and temporal vegetation variability but also allows identifying the impact of weather on vegetation [25,30]. However, care is needed with unusual extreme events. For example, if most of the NDVI values in a particular location are close to the minimum and there is an unusual event with high NDVI values, most of the calculated VCI will be very low. Also, NDVI are hindered by noise arising from varying atmospheric conditions and sun-sensor-surface viewing geometries [40–43], to minimize the possible impacts of undetected clouds and poor atmospheric conditions [41] a smoothing technique should be applied [40–43]. To overcome this issue, Klishch and Atzberger [41] estimates uncertain for NDVI values, which is used to downweight uncertain observation while calculating VCI. Moreover, the VCI in the present study was calculated at a 250 m spatial resolution to monitor and evaluate agricultural drought, which would be useful because of the geographic and agricultural conditions of the BioBío in Chile (Figure 1).

The SPI is a multiscale drought index that could be used to measure short-term rainfall deficit related to agricultural drought; this is not always true because agricultural drought is mainly affected by soil moisture stress [44] which depends on rainfall as well as many other factors. The VCI is a more direct measurement of agricultural drought because it reflects vegetation health scaled according to long-term NDVI variability for the period under study. Some authors [26,35,45,46] compared vegetation indices and SPI to evaluate the correlation between agricultural and meteorological drought. For example, Quiring and Ganesh [46] evaluated the usefulness of VCI to monitor meteorological drought in Texas, analyzed the relationship between VCI and SPI and its result shows that VCI is most strongly correlated with the 6-month and 9-month SPI, and showed that VCI is strongly influenced by spatially varying environmental factors. Gebrehiwot *et al.* [27] also used VCI and SPI to evaluate the spatial and temporal characteristics of vegetative and meteorological drought; they found a time lag between the peak VCI period and precipitation values obtained from the meteorological stations. Ji and Peters [47] analyzed the relationship between NDVI (derived from AVHRR) and SPI in croplands in the northern Great Plains, which have similar weather and agricultural conditions as those found in the BioBío Region, and showed that the relationship between NDVI and SPI is significant in grasslands and croplands if the seasonal effect is taken into account.

In collaboration with the Ministry of Agriculture of Chile, the Food and Agriculture Organization of the United Nations (FAO), the International Research Institute for Climate and Society (IRI), and some other government institutions and research centers, the United Nations Educational, Scientific and Cultural Organization (UNESCO) implemented the Chilean Agroclimatic Observatory (www.climatedatalibrary.cl), which collects different meteorological, hydrological, and agricultural information as well as various indices to monitor drought and support decision makers when Chile faces drought conditions.

The present study evaluated the VCI drought index proposed by Kogan [39], calculated it from a time series of MODIS data, and applied it in the BioBío Region. The VCI is compared to SPI at different time scales to identify how long would be the monthly rainfall deficit that has the major impact on agricultural drought in the region. Additionally, the usefulness of monitoring

agricultural drought is assessed by comparing VCI with the agricultural drought emergency declared by the Chilean government in the study area. The aim of this study was to assess VCI derived from MODIS data at 250 m spatial resolution as an effective indicator for monitoring agricultural drought and evaluate its observed impact in the region over the last 16 years. Based on this analysis, recommendations are made to include the index in the Chilean Agroclimatic Observatory to support climate-informed decision making.

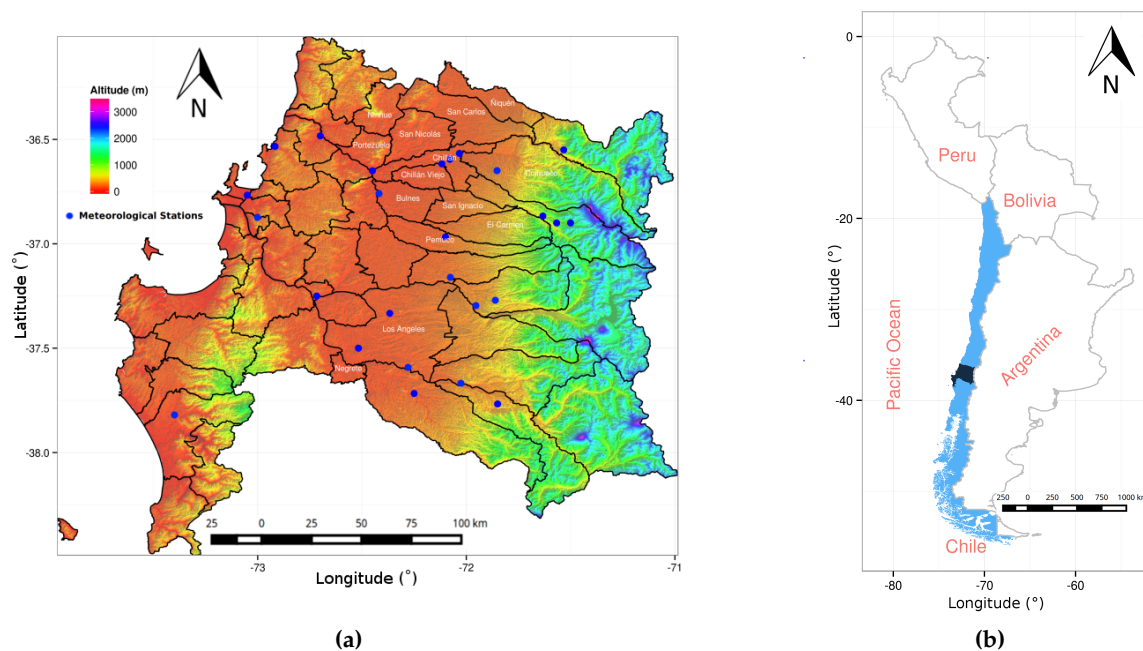


Figure 1. Study area. (a) BioBío Region administrative units in a digital terrain model with 26 weather stations; (b) Location of the BioBío Region, Chile.

2. Study Area

The BioBío Region in Chile is located between $36^{\circ}00'$ and $38^{\circ}30'$ south latitude and between $71^{\circ}00'$ and $74^{\circ}00'$ west longitude along the South Pacific Ocean (Figure 1b) with a total area of $37,068.7 \text{ km}^2$. This area is characterized by the transition from a warm Mediterranean climate to a humid and temperate climate. In terms of agricultural, this region produces a significant amount of annual crops, including wheat, oats, barley, sugar beet and corn, which have a growing season between September and April. The region has 54 administrative units (Figure 1a).

The bioclimatic variables estimated by Hijmans *et al.* [48] were used to describe the spatial climatic characteristics of the study area. These variables were derived from monthly temperature and rainfall values to generate more biologically meaningful variables. Precipitation in the driest month is generally $< 35 \text{ mm}$ and a significant portion of the region has $< 20 \text{ mm}$ rainfall in that month (Figure 2). The wettest month has precipitation between 150 mm and 350 mm while total annual precipitation is between 750 mm and 2000 mm . The temperature in the warmest month is over 25°C mainly in the central part of the region, as shown in Figure 3. The temperature in the coldest month is between 0°C and 7°C from the center to the west and below 0°C to the east and the annual mean temperature is usually above 10°C .

Based on land cover (MCD12Q1.51), changes in the cropland area for the main administrative units are shown in Table 1. In general, the cropland area decreased from 2001 to 2013, and the administrative units of San Nicolas and Chillán Viejo showed the largest changes. The land cover map (2013) for the region, illustrated in Figure 4, indicates that most of the region is covered by forest and this is followed by cropland and grassland.

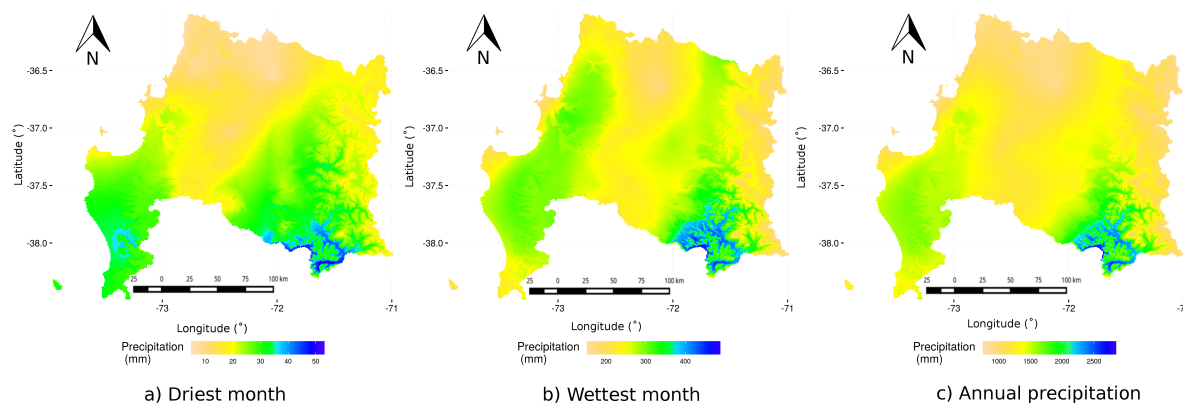


Figure 2. Bioclimatic precipitation variables of the BioBío Region, Chile. (a) Driest month; (b) Wettest month; (c) Annual precipitation.

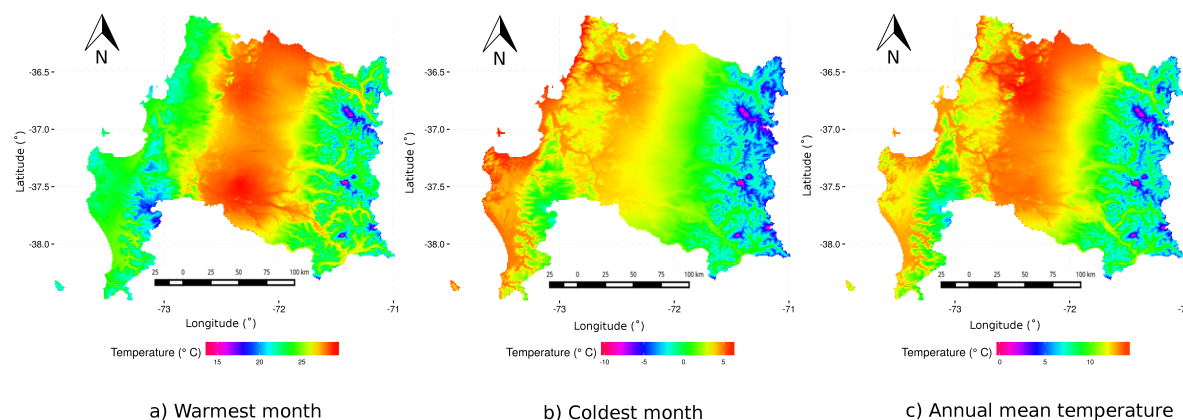


Figure 3. Bioclimatic temperature variables of the BioBío Region, Chile. (a) Driest month; (b) Wettest month; (c) Annual mean temperature.

Table 1. Percentage of cropland area (%) of 15 administrative units of the BioBío Region, Chile, with cropland area $\geq 10\%$ from 2001 to 2013 and the 13-year mean.

No.	Adm. Unit	2001	2002	2003	2004	2005	2006	2007	2008	2009	2010	2011	2012	2013	$\bar{X}_{2001-2013}$
1	San Ignacio	79	79	80	78	77	73	73	72	76	76	73	73	76	76
2	Bulnes	82	81	80	78	77	76	76	76	76	75	73	72	73	77
3	San Carlos	79	74	71	66	67	66	68	65	76	74	71	62	68	70
4	Chillán	73	71	71	66	66	64	64	62	66	66	63	59	63	68
5	Ñiquén	76	68	63	54	53	55	57	59	72	71	63	54	59	62
6	El Carmen	54	55	54	52	51	50	50	46	48	46	44	45	46	47
7	Chillán Viejo	65	61	61	55	52	46	49	44	58	55	53	39	42	48
8	San Nicolás	77	63	56	45	45	46	49	45	64	59	54	36	40	52
9	Negrete	57	59	51	47	41	47	42	49	54	43	37	35	47	52
10	Los Angeles	31	34	32	32	26	28	26	27	30	25	22	25	32	29
11	Coihueco	26	26	25	23	22	20	19	19	21	21	20	19	20	28
12	Pemuco	37	37	37	33	31	25	26	24	27	25	23	18	21	22
13	Yungay	24	26	24	22	20	19	20	18	20	18	16	14	17	20
14	Quillón	31	24	20	14	16	16	15	15	20	17	16	12	15	18
15	Pinto	18	16	14	13	13	12	12	11	12	12	11	10	11	13

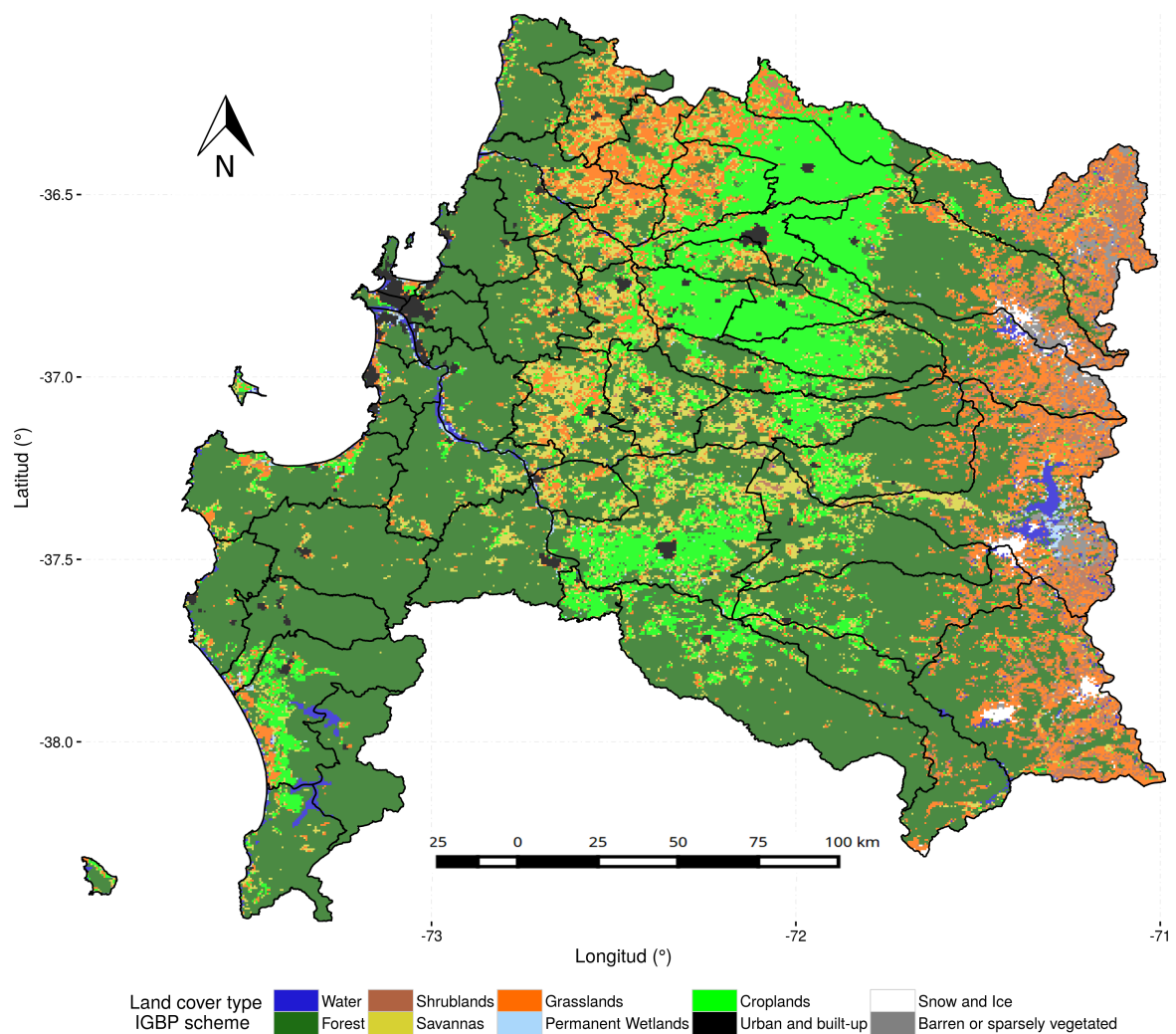


Figure 4. Land cover classes in the BioBio Region, Chile, based on the IGBP land cover scheme for the MODIS MCD12Q1 version 5.1 product.

3. Data

The MODIS has been a key environment remote sensing tool for more than 16 years; it has been used in countless studies of different disciplines all over the world. The MODIS instrument was developed to improve heritage sensors in terms of its spectral, spatial, and temporal resolutions, as well as more stringent calibration requirements. This instrument takes observations in 36 spectral bands covering wavelengths from 0.41 to 14.4 μm and at three nadir spatial resolutions: 250 m, 500 m, and 1 km [49].

The usefulness of NDVI for evaluating vegetation response is well known [50]. In the present case, the vegetation indices (VI) were obtained from the MODIS 'Vegetation Indices 16-Day L3 Global 250 m' short name 'MOD13Q1' product [51]. Huete *et al.* [50] present the NDVI analysis and the Enhanced Vegetation Index (EVI); their results demonstrate the scientific usefulness of MODIS VI. Moreover, Miura *et al.* [52] compared MODIS VI with the high-resolution Advanced Thermal Emission and Reflection Radiometer (ASTER) (15 m) and showed that they coincided well on a global scale.

Several land cover products are available; the most frequently used are GLC-2000 [53], Globcover [54], and MODIS Collection 5 land cover [55]. Comparative studies have shown large spatial discrepancies among these three products. Two of the main advantages of the MODIS

Collection 5 are its 500 m spatial resolution and, according to Friedl *et al.* [55], the product overall accuracy is approximately 75%. Therefore, the MODIS cropland cover 'Land Cover Type Yearly L3 Global 500 m SIN Grid' short name 'MCD12Q1' version 5.1 was used. Data for the present study were obtained through the online Data Pool at the NASA Land Processes Distributed Active Archive Center (LP DAAC) and USGS/Earth Resources Observation and Science (EROS) Center, Sioux Falls, South Dakota (https://lpdaac.usgs.gov/get_data).

Meteorological data were collected from 53 meteorological stations in the BioBío Region from the General Water Authority (DGA) and the Chilean Meteorological Directorate (DMC). A total of 26 stations were selected from this dataset; stations had more than 30 years of records and few missing data (Figure 1).

4. Methods

4.1. Procedure for Calculating VCI in Cropland Areas

A time series of vegetation index products (MOD13Q1 version 5) was used to derive the VCI index, and the land cover product (MCD12Q1 version 5.1) [55] was used to determine the spatial extension of croplands; both products are from the Moderate-Resolution Imaging Spectroradiometer (MODIS) sensor. Meteorological stations with a long record (more than 30 years) were used to calculate the SPI index.

All processing and calculations with the raster data were performed with the R software [56] and the 'raster' package [57]. Once the MOD13Q1 and MCD12Q1 satellite data were obtained, they were reprojected to the WGS84 datum and geographic projections with the Modis Reprojection Tool (MRT) [58] using nearest neighbor resampling. A smoothing process was required to reduce noise in the NDVI time series. Multiple techniques are available in the literature to do this [40–43]. In the present case, a locally-weighted polynomial regression (Lowess) [59] was used. Figure 5, shows time-series of NDVI compared with those smoothed by Lowess. In future studies the smoothing could be improved using for example an adapted lowess [60] or also with a modified Whittaker smoother as proposed by Klisch and Atzberger [41].

Then, with the smoothed NDVI, $NDVI_{max}$, and $NDVI_{min}$ from 2000–2015, the VCI values were calculated using Equation (1) for each pixel in the BioBío Region every 16-day. Finally, the VCI time series (2000–2015) were masking out, using the cropland mask.

4.2. Cropland Mask

The 'cropland' type in the present study is the IGBP classification scheme of the MCD12Q1 collection 5.1, and it was used because cropland class reliability is > 92% according to Friedl *et al.* [55]. In addition, the cropland mask derived from IGBP scheme concurs well with the cropland data from the 2007 national agriculture and livestock census [61]. From the MCD12Q1 product, the land cover class that corresponds to croplands (class 12 and 14 of the IGBP scheme) was used to create an agricultural mask with a 500 m spatial resolution for the 2001–2013 period. These data had to be resampled from a 500 m to 250 m spatial resolution using the 'raster' package [57] to coincide with the VCI resolution. Thirteen yearly cropland masks were created; the mask for 2001 was used with VCI data for 2000 and 2001, and the mask for 2013 was used for 2013, 2014, and 2015. A sub-selection of 15 units with >10% cropland was established from the total of 54 administrative units.

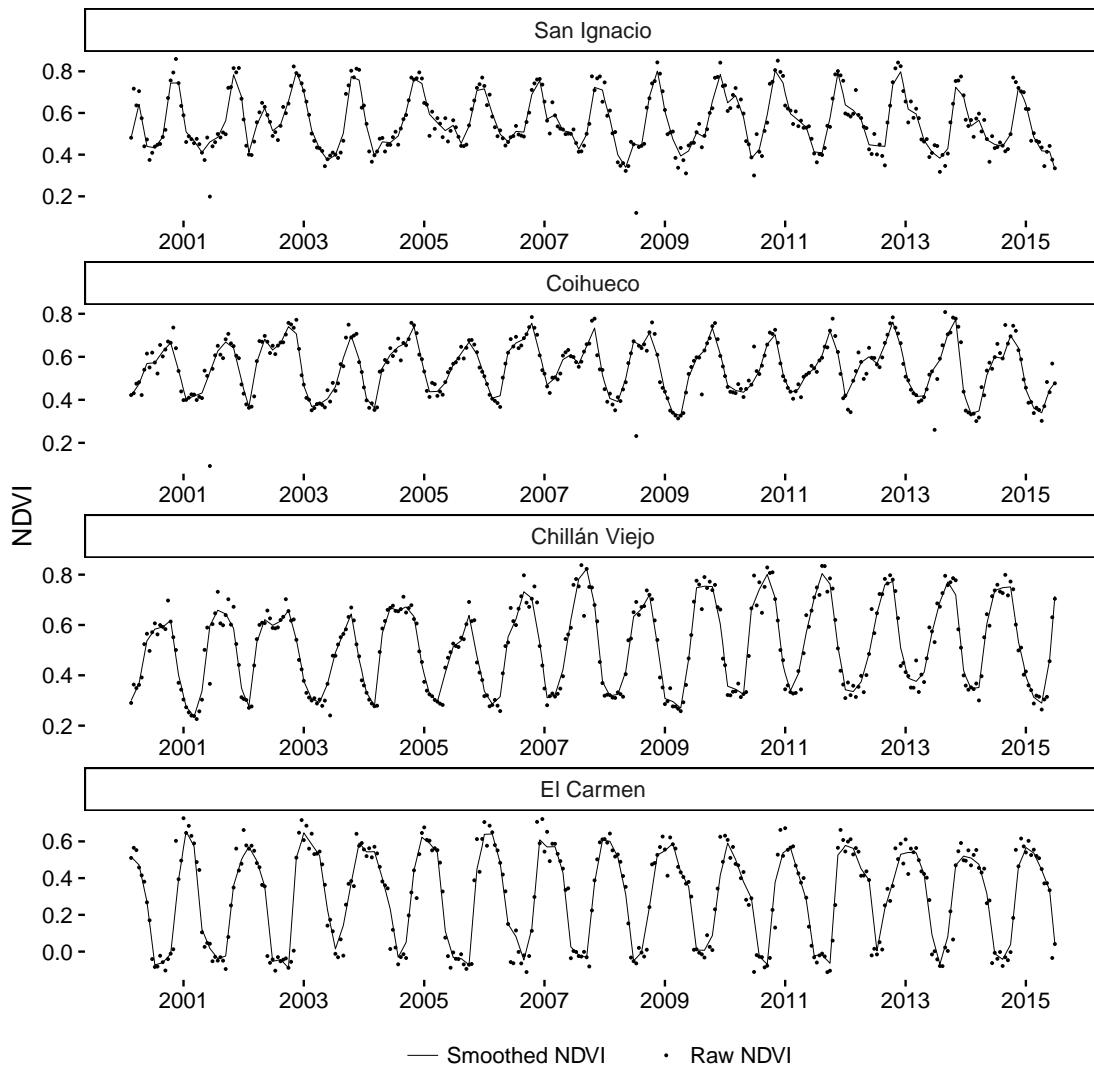


Figure 5. Time-series comparison between raw NDVI (points) and smoothed NDVI by Lowess (lines) for five points on five administrative units in cropland areas of the BioBío Region.

4.3. Vegetation Condition Index (VCI)

The VCI [25,39] is used to monitor agricultural drought and is derived from NDVI. It scales NDVI between its maximum and minimum values for a given period and can be expressed as:

$$VCI_{(i,p,j)} = \frac{NDVI_{(i,p,j)} - NDVI_{min(i,p)}}{NDVI_{max(i,p)} - NDVI_{min(i,p)}} \quad (1)$$

where $NDVI_{(i,p,j)}$ is the smoothed NDVI for pixel i , period p and year j ; in the present study, the period is 16-day (from 1 to 23 for each year) from 2000–2015. $NDVI_{max(i,p)}$ and $NDVI_{min(i,p)}$ are the multi-annual maximum and minimum, respectively, calculated for each pixel i and 16-day period p from 2000–2015. To compare VCI values extracted in the 26 weather stations with SPI monthly data, a weighted mean was applied to convert VCI to monthly values.

According to Kogan *et al.* [62], NDVI represents two environmental signals, the ecosystem, which explains long-term changes in vegetation (driven by climate, soils, vegetation type, topography, *etc.*), and the weather (short-term), which explains intra- and inter-annual variations in each ecosystem

in response to weather fluctuations. Given that the weather component is much smaller than the ecosystem component, the algorithm was developed to enhance the weather component.

4.4. Standardized Precipitation Index (SPI)

Since VCI incorporates both climatic and ecological components [39], an analysis was required to understand the effect of the precipitation variability on VCI for croplands in the study area. The SPI drought index was therefore used to analyze the correlation of VCI with rainfall departure. The SPEI [8] is a more significant measure because it incorporates the temperature effect. However, in the present study, SPEI could not be used because of a scarcity of temperature measurements; this situation did not allow calculating reference ET in each one of the weather stations.

The SPI [6] is a meteorological drought index that is estimated from long-term precipitation records. These long-term records are fitted to a probability distribution (usually Gamma or Pearson III) which is then transformed into a normal distribution so that mean SPI for the location and desired period is zero. Positive SPI values indicate that precipitation is higher than the median while negative values indicate precipitation is lower than the median. The SPI can be computed for different time scales where shorter scales (1–6 months) are related to short-term deficit, such as soil water content (vegetation response) and longer scales (12–36 months) with a long-term deficit that is generally associated with groundwater and reservoirs. The ‘spi’ function from the ‘SPEI’ R package [63] was used to calculate SPI for time scales between 1 and 6 months for the 26 meteorological stations. To fit a ‘Gamma’ distribution on the data, the ‘spi’ function was set by the method of unbiased probability weighted moments.

The classification scheme used for VCI and SPI was similar to the classification scheme used by Bhuiyan *et al.* [64] and proposed by Du *et al.* [36], as shown in Table 2.

Table 2. Drought classification scheme for SPI and VCI ([36,64]).

Drought Classes		SPI		VCI	
Extreme		SPI < −2.0		0 ≤ VCI < 10	
Severe	−2.0 ≤	SPI < −1.5		10 ≤ VCI < 20	
Moderate	−1.5 ≤	SPI < −1.0		20 ≤ VCI ≤ 30	
Mild	−1.0 ≤	SPI < 0.0		30 ≤ VCI ≤ 40	
No drought	0.0 <	SPI		40 < VCI ≤ 100	

4.5. Correlation between VCI and SPI

The standardized VCI anomalies were used for the Pearson correlation test:

$$STD_{ijk} = \frac{X_{ijk} - \bar{X}_{ij}}{\sigma_{ij}} \quad (2)$$

where X_{ijk} is the VCI value in pixel i , period j and year k , \bar{X}_{ij} is the mean value of VCI in pixel i and period j ; and σ_{ij} is the standardized deviation of pixel i and period j .

To identify the lag-time period that is more sensitive to rainfall deficit, the correlation between standardized VCI and SPI for the cropland area of the BioBío Region for three different seasons was tested: (1) January to December; (2) September to April (growing season); and (3) November to April (modified growing season). A modified growing season was tested because when is considered the normal growing season (September–April), and SPI-3 is calculated in September (start of growing season), it refers to the accumulated effect of rainfall deficit from July to September. Instead, if is considered the start of the period in November (start of modified growing season), then the SPI-3 reflect the rainfall deficit from September to November. In this way, is possible evaluate the impact of rainfall deficit which occurs during the months of the growing season.

5. Results and Discussion

5.1. Spatio-Temporal Variation of VCI and Comparison with Drought Declaration

At the regional level, the variation of drought intensity percentages in the study area for the cropland area between the 2000/2001 and 2014/2015 growing seasons is illustrated in Figure 6a. The BioBío Region reached the lowest percentage of the cropland area under drought in 2006/2007 (17%) and the highest in 2008/2009 (55%). The 2007/2008 and 2008/2009 periods exhibited almost the same percentage of cropland surface under drought; however, a difference was observed in the extreme intensity class covering more cropland surface in 2008/2009 (14%), compared to the 2007/2008 period (11%). Figure 6b depicts the box-plot of mean VCI values in the BioBío Region considering the cropland growing season. The box-plot shows the upper and lower quartiles (Q3 and Q1) and the median value. The 2007/2008 and 2008/2009 periods showed the lowest VCI values, followed by 2014/2015 (Figure 6a). Moreover, 2008/2009 had 75% of its values with VCI < 32% and 50% of the data had VCI values between 21% and 32%, causing it to be the most severe period, which was noted by a considerable increase of the surface under extreme drought.

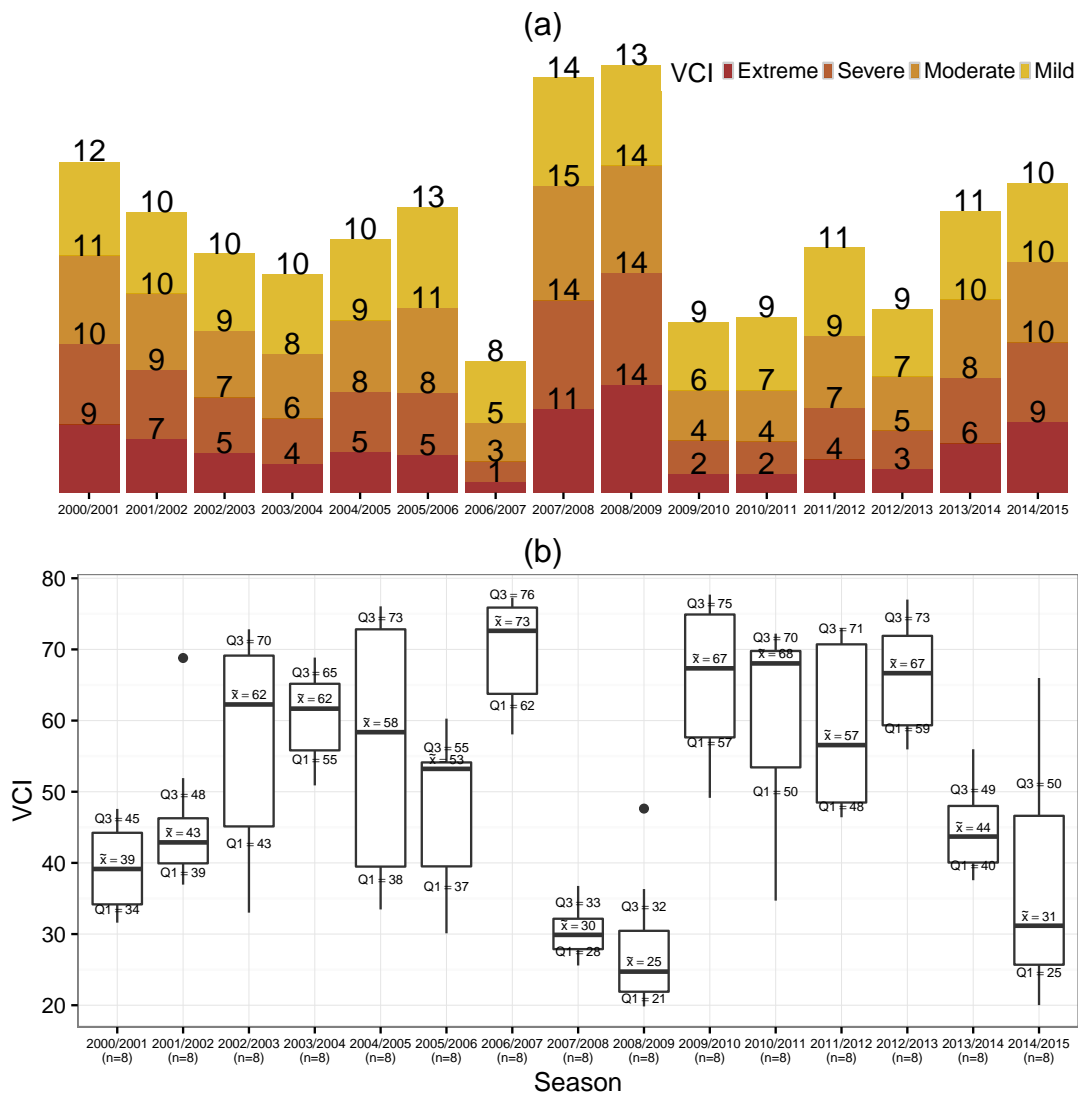


Figure 6. Variation of the (a) global VCI percentage (%) of cropland surface with different VCI classes and (b) boxplot of global VCI intensity (%) for the growing seasons between 2000/2001 and 2014/2015 in the Biobío Region, Chile.

On the administrative unit level, Figure 7 illustrates a heatmap of the time series VCI intensity values on the cropland surface (Figure 7a,c) and the percentage of cropland surface under drought conditions ($VCI \leq 40$) (Figure 7b,d) for 15 administrative units between 2007–2009 and 2014–2015. The dashed white line corresponds to the times in the past 16 years when the Chilean government has declared an agricultural drought emergency in the region. According to the VCI values, the administrative unit was under moderate and mild drought conditions between 2007 and 2008 while in the late growing season from January to May, VCI intensity was mostly moderate drought, and the surface percentage of drought was $>60\%$ for each administrative unit. At the beginning of February 2008 (2007/2008 season) the government declared an agricultural drought emergency. However, during the next season, 2008/2009, drought conditions were similar but with a longer duration (September–May) and more severe intensity, but the government did not declare drought emergency. The last drought emergency was declared in March 2015 and it seems that it was declared late according to VCI intensity and cropland surface affected. As displayed in Figure 7b, the emergency was declared in the middle of the drought period (January–May) when the percentage of surface affected by drought was between 60% and 90%. The drought emergency declared by the Ministry of Agriculture of Chile do not consider the intensity levels but rather only the conditions with or without drought.

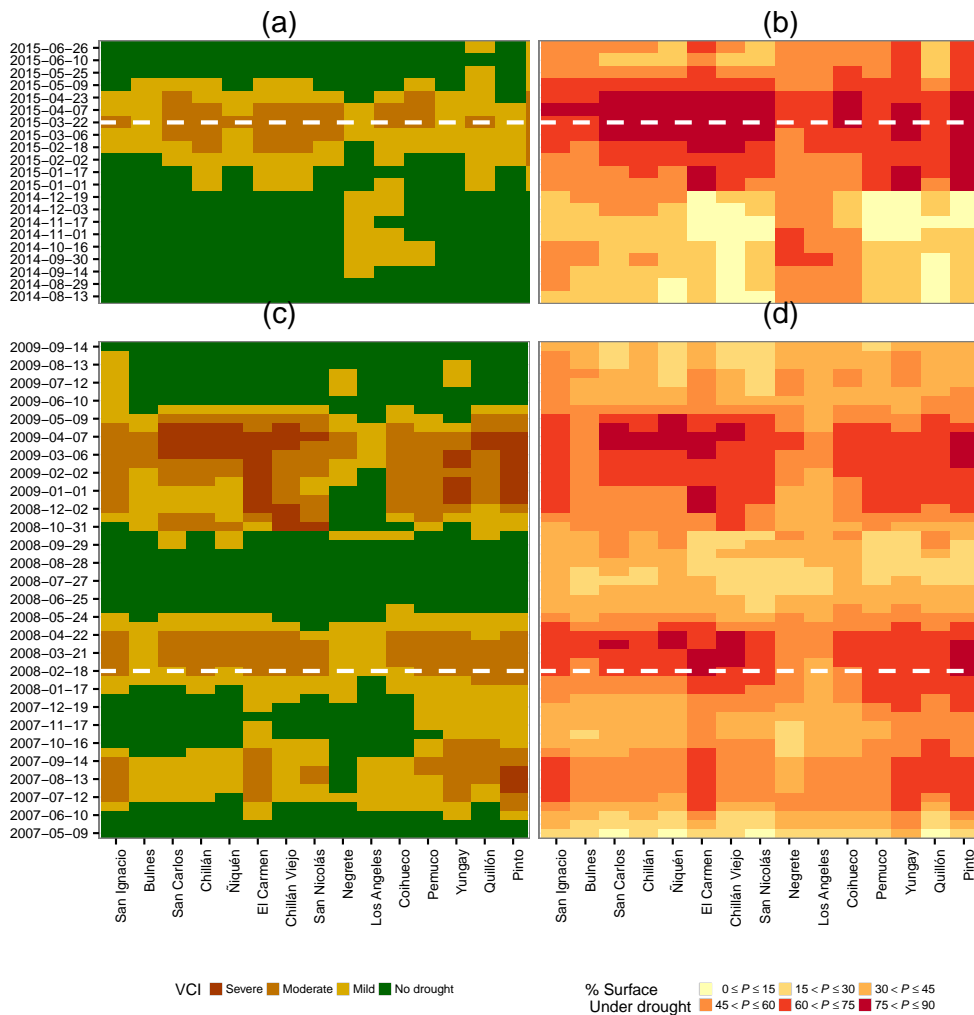


Figure 7. Heatmap of VCI intensity and percentage of cropland area $< VCI = 40$ in the main cropland administrative units in the study area. (a) Intensity and (b) Surface under drought for the 2014–2015 season; (c) Intensity and (d) Surface under drought for 2007–2009 season. The dashed white line corresponds to the date when the agricultural drought emergency was declared by decision makers.

The periods with the lowest VCI means for each unit during the growing seasons in the last 16 years are mapped in Figure 8. Figure 8a shows that the 2000/2001 season had partial drought conditions, which mostly affected the western part of the region, with three, eight, and nine units with severe, moderate, and mild drought conditions, respectively. It is possible to note that the 2007/2008 and 2008/2009 seasons had drought conditions in almost every unit in the region with mild and moderate drought intensity as the main condition. These periods also had a unit surface percentage under drought > 45% (Figure 8b). The 2014/2015 season had mostly a surface percentage between 30% and 45% under drought conditions in each unit, also had two and nine units with moderate and mild drought, respectively.

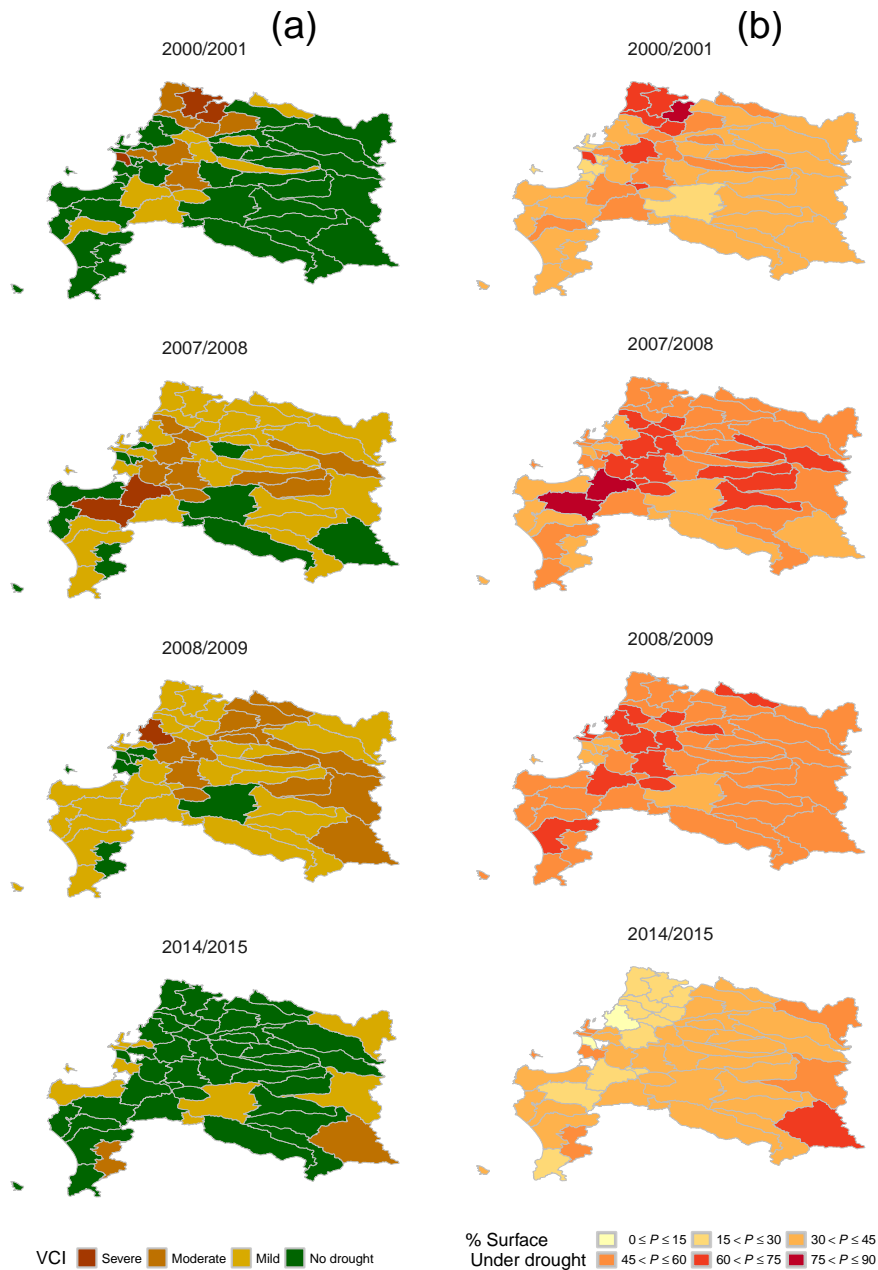


Figure 8. (a) Mean VCI conditions and (b) percentage of cropland surface with VCI ≤ 40% in the administrative units of the Biobío Region, Chile, for the 2000/2001, 2007/2008, 2008/2009, and 2014/2015 growing seasons (September–April).

The VCI temporal mean at pixel level for the 2007/2008, 2008/2009, and 2014/2015 growing seasons (September–April) in the cropland area of the BioBío Region is shown in Figure 9.

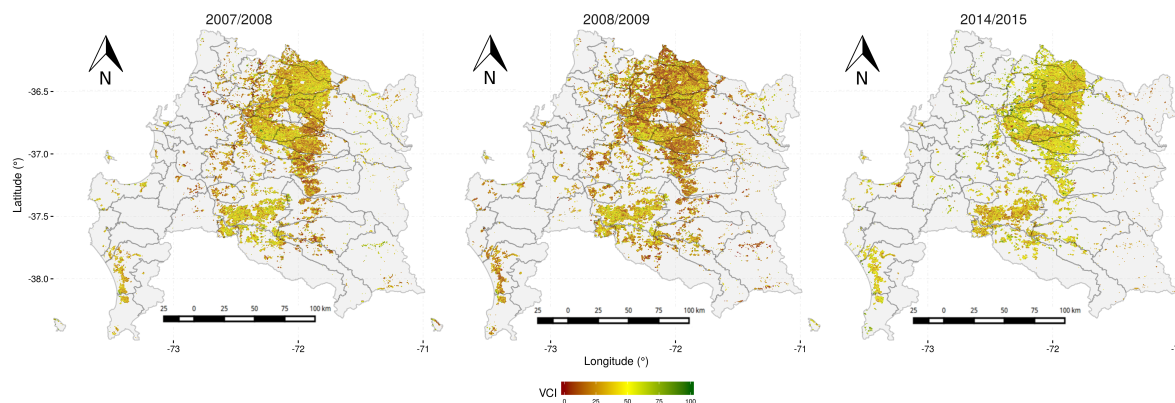


Figure 9. VCI mean values for croplands during growing season (September–April) in the BioBío Region, Chile, for 2007/2008, 2008/2009, and 2014/2015 seasons.

5.2. Correlation VCI vs. SPI

Globally, in the BioBío Region we compared three averaged periods (September–April, November–April, and January–December) and the correlation between SPI and VCI at different time scales. We found the highest regional correlation between SPI-3 and VCI during the growing season (September–April); with a Pearson correlation value of 0.54. The period between November and April shows a higher Pearson correlation value of 0.63. This is comparable to the results presented by Vicente-Serrano [34], who indicated that the vegetative drought index is useful for monitoring drought during the growing season.

The administrative units with a cropland area > 10% were correlated with the nearest meteorological station. Pearson correlation values for SPI-1 to SPI-6 are listed in Table 3. As previously shown, the higher correlation values were at SPI-3 (0.40 to 0.78) (Table 3). Vegetation had a short-term response to rainfall, and 3-month departures explained between 16% and 61% of the variance in cropland health. Mean VCI anomaly and SPI-3 values were compared in Figure 10 for the period between November and April (modified growing season). The SPI-3 and VCI values were negative and similar for all 15 administrative units in the 2007/2008, 2008/2009, and 2014/2015 seasons, which corresponded to the three periods in the last 16 years in which the BioBío Region was under the most severe drought conditions (Figure 6). However, there was an opposite correlation with negative VCI and positive SPI-3 in the 2000/2001 season. Rainfall is the main variable among others affecting vegetation response. Management, irrigation, and plant disease also affect agricultural drought, and they must be analyzed in greater detail.

Monthly correlation values calculated at 26 weather stations during the growing season are displayed in Figure 11a; September and October (beginning of the season) showed the lowest correlation between SPI-3 and VCI whereas from November to April (middle and end of season) the Pearson correlation value was always >0.6; the lowest value during this period was in February. The correlation of VCI with SPI-1 was the highest in October, November, and February; and with SPI-3 the correlation was around ≈ 0.6 from November to March. This indicated that rainfall deficit in September and October had a higher impact on vegetation with an accumulated effect beginning in November during the growing season. On the other hand, rainfall during July, August, and September had a lower impact on the agricultural drought conditions in September and October. The period from November to April was therefore identified as being more sensitive to water scarcity

because of the accumulated effect of three months of rainfall on the cropland growing season. This result concurs with observations by Ji and Peters [47], who found that the correlation between vegetation and SPI-3 was stronger in the middle of the season and weaker at the beginning and end of the growing season. Cropland vegetation in this region mainly had a short-term response (3 months) to rainfall deficit. In terms of the monthly rainfall deficit (SPI-1), October, November, December, and February were more significant with Pearson correlation values of 0.49, 0.49, 0.43, and 0.48, respectively. The 6-month accumulated effect of rainfall deficit on vegetation (SPI-6), which began increasing in December and peaked in April, confirms the accumulated effect from November to April ($r = 0.68$). In addition, if we want to monitor the croplands in more detail, we could consider SPI-1 in October, SPI-3 from November to February, and SPI-6 in March and April.

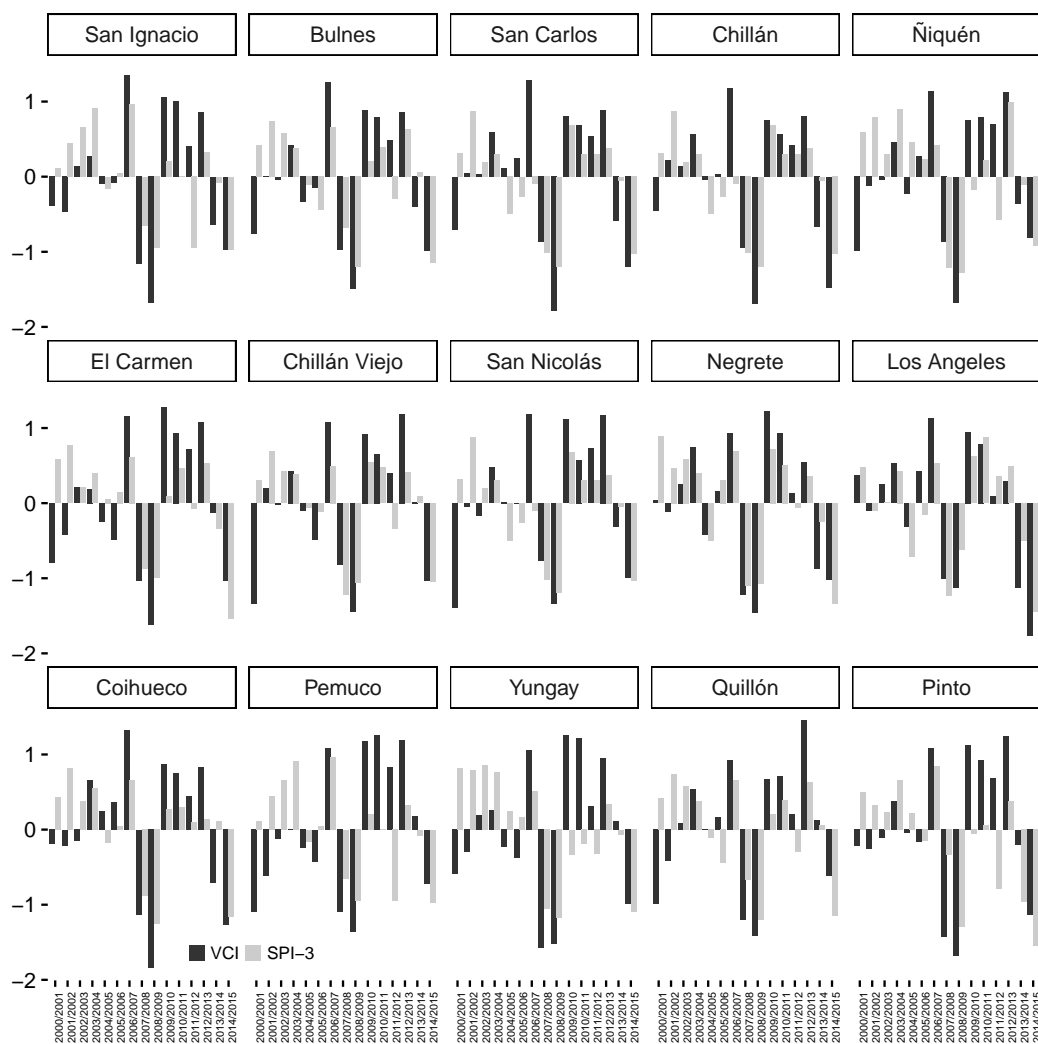


Figure 10. Comparison of SPI-3 and VCI anomaly for 15 administrative units with percentage cropland > 10% from 2000/2001 to 2014/2015 modified growing seasons (November–April).

Comparative results of correlations between VCI and SPI time scales of 1 to 6 months for three periods and four meteorological stations are shown in Figure 11b. The pattern is similar for all the periods and November to April had the highest Pearson correlation between SPI and VCI. This correlation peaked at the 3- or 4-month time scales and then decreased. However, for the station with lower correlations (‘San Carlos de Puren’), the SPI-4 showed clearly the highest correlation. The SPI-3 in the ‘Quilaco’ station was prominent with $r = 0.77$.

Table 3. Pearson correlation value (r) between time scale 1 to 6 and standardized VCI for 15 administrative units in the BioBío Region, Chile, with cropland area > 10% and considering the mean values between November and April.

No.	Adm. Unit	Station Name	SPI-1	SPI-2	SPI-3	SPI-4	SPI-5	SPI-6
1	Los Angeles	DGA Las Achiras	0.46	0.69	0.78	0.73	0.67	0.64
2	Chillán	DMC Chillán	0.38	0.56	0.70	0.66	0.59	0.53
3	Bulnes	DGA Chillancito	0.37	0.59	0.66	0.59	0.47	0.34
4	Negrete	DGA Los Angeles	0.47	0.69	0.74	0.69	0.62	0.55
5	Chillán Viejo	DGA Chillán Viejo	0.41	0.59	0.67	0.64	0.55	0.45
6	El Carmen	DGA Diguillin	0.29	0.48	0.58	0.55	0.46	0.36
7	San Ignacio	DGA Pemuco	0.31	0.48	0.56	0.51	0.43	0.36
8	San Nicolás	DMC Chillán	0.31	0.47	0.56	0.53	0.47	0.39
9	San Carlos	DMC Chillán	0.34	0.49	0.59	0.56	0.50	0.45
10	Pinto	DGA Las Trancas	0.24	0.40	0.49	0.45	0.35	0.29
11	Coihueco	DGA Coihueco	0.33	0.49	0.58	0.52	0.43	0.38
12	Yungay	DGA Cholguan	0.19	0.37	0.43	0.44	0.40	0.33
13	Pemuco	DGA Pemuco	0.21	0.34	0.40	0.37	0.29	0.18
14	Quillón	DGA Chillancito	0.38	0.55	0.62	0.59	0.51	0.37
15	Ñiquen	DGA San Fabián	0.38	0.55	0.57	0.48	0.38	0.28

Correlation is significant at 0.01.

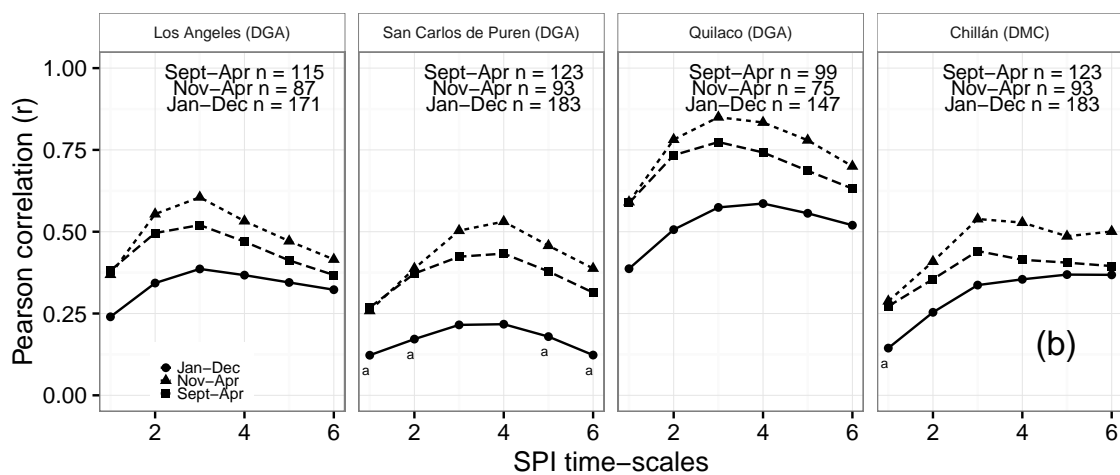
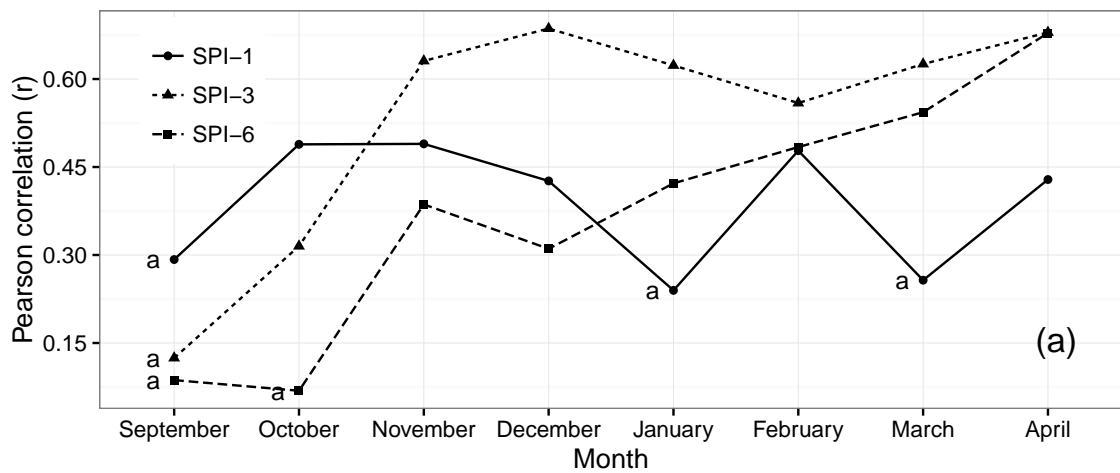


Figure 11. (a) Correlation between mean VCI (croplands) and mean SPI at time scales between 1 to 6 for meteorological station Number 4 in the Biobío Region, Chile, for three different periods; (b) Monthly correlation between SPI-1, SPI-3 and SPI-6 with VCI in the growing season. Letter (a) in the plot means significance at $p > 0.01$.

Several studies have compared the vegetation drought index with meteorological conditions [27,45–47,65]. Our observations are consistent with those of Gebrehiwot *et al.* [27], who found a strong correlation between VCI and precipitation deficit of the last 3 months at the station and regional levels. Similarly, Bajgiran *et al.* [65] established the highest correlation with 3-month precipitation in stations where land use is predominantly cropland ($r = 0.8$) and grassland (0.81). Ji and Peters [47] indicated a Pearson correlation value of 0.47 between VCI and SPI-3 for the croplands of the northern Great Plains, and Wu *et al.* [45] found a very good correlation between VCI and SPI-3 for grassland. Quiring and Ganesh [46] identified the correlation between SPI and VCI in Texas as having high spatial variability; however, they found that VCI is most strongly correlated with the 6-month and 9-month SPI. They also established permeability, irrigation, landcover type and water table depth as the most important independent variables besides rainfall, which explain the variation in vegetation health [46].

It will be important to consider the effect of temperature on agricultural drought in future studies by using, for example, SPEI [8]; this is a multiscalar drought index which takes into account potential ET as a measurement of water demand. This was not possible in the present study because historical temperature data were scarce. One option to overcome the lack of temperature data could be the use of remote sensing data, such as the MOD16 ET product proposed by Mu *et al.* [66].

6. Conclusions

In a country where the impact of agricultural drought is increasing, detailed monitoring and early warning tools are required to trigger responses that allow mitigating the drought effect. Therefore, a thorough understanding of the drivers of agricultural drought are needed even when detailed field observations are lacking and meteorological stations are scarce, as is the case in Chile. This result makes remote sensing datasets for vegetation monitoring a particularly powerful tool under these circumstances.

The present study assessed the agricultural drought dynamics using the vegetation condition index (VCI) at 250 m spatial resolution and evaluated the cropland area of the BioBío Region in Chile from 2000 to 2015.

A VCI analysis for croplands could identify the spatial distribution of stressed vegetation associated with drought conditions. Comparing cropland VCI for all the administrative units during the growing stage indicated that, according to the selected drought intensity classification, three drought episodes have occurred in the last 16 years that coincide with the years in which agricultural emergency funding was provided to the farmers in the region. The VCI indicator shows the potential to further tailor the drought emergency response and identifies more objectively the stakeholders who are the most affected even when detailed local observations are lacking.

The correlation between rainfall deficit (SPI) on short- and long-term scales and VCI values shows that SPI-3 exhibited the highest correlation values for the BioBío Region between November and April, defined as a modified growing season, instead of between September and April, which is the normal growing season. This result indicates that vegetation responds rapidly to rainfall deficit beginning in September and this is evidenced in vegetation in November.

Based on these findings, we can conclude that VCI is useful for monitoring agricultural drought in the BioBío Region and is closely correlated with SPI-3 during the modified growing season (November to April), which indicate that rainfall deficit beginning on September it is when has a larger impact on vegetation health, this would be related with crops types in the region, what it should be evaluated in future studies. This makes it a relevant indicator for agricultural drought monitoring and response plans. Further research is needed to associate the remote sensing values observed at high resolution (250 m) with the measured crop yield [67] and individually identify more detailed crop responses. This identification will gradually construct an effective drought management tool for the agricultural sector in Chile.

Acknowledgments: We would like to express our gratitude to the 'Unidad Nacional de Emergencias Agrícolas de Chile' (National Agricultural Emergency Unit, UNEA), the 'Instituto de Investigaciones Agropecuarias' (National Institute of Agricultural Research, INIA) and the UNESCO International Hydrological Programme (IHP). The agreement between these institutions allowed developing products for Agricultural Risk Management and Agroclimatic Emergency. Also, thanks for the support to the International Centre for Eremology, Department of Soil Management from Ghent University and to the Water Research Center for Agriculture and Mining (CRHIAM, CONICYT-FONDAP-15130015). Finally, special thanks to the four anonymous reviewers, to the editor Anton Vrieling and other anonymous editor for their valuable comments, which helped to improve the quality of the manuscript. This study was funded by the CONICYT Scholarship/National Ph.D. 21141028.

Author Contributions: Francisco Zambrano and Mario Lillo-Saavedra conceived and designed the study; Francisco Zambrano conducted the data processing; Francisco Zambrano, Mario Lillo-Saavedra, Octavio Lagos, and Koen Verbist all contributed to the data analysis and writing of this manuscript. Koen Verbist, also contributed with key ideas for the analysis, presentation of results and to write the manuscript, giving better projection to the study.

Conflicts of Interest: The authors declare no conflict of interest.

References

1. Dore, M.H. Climate change and changes in global precipitation patterns: What do we know? *Environ. Int.* **2005**, *31*, 1167–1181.
2. IPCC. *Climate Change 2013: The Physical Science Basis. Contribution of Working Group I to the Fifth Assessment Report of the Intergovernmental Panel on Climate Change*; Cambridge University Press: Cambridge, UK; New York, NY, USA, 2013; p. 1535.
3. Wilhite, D.A.; Glantz, M.H. Understanding: The Drought Phenomenon: The Role of Definitions. *Water Int.* **1985**, *10*, 111–120.
4. Niemeyer, S. New drought indices. *Opt. Méd.* **2008**, 267–274.
5. Amin, Z.; Rehan, S.; Bahman, N.; Faisal, K. A review of drought indices. *Environ. Rev.* **2011**, *19*, 333–349.
6. McKee, T.B.; Doesken, N.J.; Kleist, J. The relationship of drought frequency and duration to time scales. In Proceedings of the International 8th Conference on Applied Climatology, Anaheim, CA, USA, 17–22 January 1993; pp. 179–184.
7. Mishra, A.K.; Singh, V.P. A review of drought concepts. *J. Hydrol.* **2010**, *391*, 202–216.
8. Vicente-Serrano, S.M.; Beguería, S.; López-Moreno, J.I. A multiscalar drought index sensitive to global warming: The standardized precipitation evapotranspiration index. *J. Clim.* **2010**, *23*, 1696–1718.
9. Palmer, W.C. *Meteorological Drought; Research Paper No. 45*. US Department of Commerce, Weather Bureau: Washington, DC, USA, 1965.
10. Alley, W.M. The palmer drought severity index: Limitations and assumptions. *J. Clim. Appl. Meteor.* **1984**, *23*, 1100–1109.
11. Palmer, W.C. Keeping track of crop moisture conditions, nationwide: The new crop moisture index. *Weatherwise* **1968**, *21*, 156–161.
12. Shafer, B.A.; Dezman, L.E. Development of a Surface Water Supply Index (SWSI) to Assess the Severity of Drought Conditions in Snowpack Runoff Areas. In Proceedings of the Western Snow Conference, Fort Collins, CO, USA, 19–23 April 1982, pp. 164–175.
13. Vicente-Serrano, S.M.; López-Moreno, J.I.; Beguería, S.; Lorenzo-Lacruz, J.; Azorin-Molina, C.; Morán-Tejada, E. Accurate computation of a streamflow drought index. *J. Hydrol. Eng.* **2012**, *17*, 318–332.
14. Caccamo, G.; Chisholm, L.; Bradstock, R.; Puotinen, M. Assessing the sensitivity of MODIS to monitor drought in high biomass ecosystems. *Remote Sens. Environ.* **2011**, *115*, 2626–2639.
15. Wu, J.; Zhou, L.; Liu, M.; Zhang, J.; Leng, S.; Diao, C. Establishing and assessing the Integrated Surface Drought Index (ISDI) for agricultural drought monitoring in mid-eastern China. *Int. J. Appl. Earth Obs. Geoinf.* **2013**, *23*, 397–410.
16. Rojas, O.; Vrieling, A.; Rembold, F. Assessing drought probability for agricultural areas in Africa with coarse resolution remote sensing imagery. *Remote Sens. Environ.* **2011**, *115*, 343–352.
17. Rhee, J.; Im, J.; Carbone, G.J. Monitoring agricultural drought for arid and humid regions using multi-sensor remote sensing data. *Remote Sens. Environ.* **2010**, *114*, 2875–2887.

18. Logan, K.; Brunsell, N.; Jones, A.; Feddema, J. Assessing spatiotemporal variability of drought in the U.S. central plains. *J. Arid. Environ.* **2010**, *74*, 247–255.
19. Kogan, F.N. Application of vegetation index and brightness temperature for drought detection. *Adv. Space Res.* **1995**, *15*, 91–100.
20. Tonini, F.; Lasinio, G.J.; Hochmair, H.H. Mapping return levels of absolute NDVI variations for the assessment of drought risk in Ethiopia. *Int. J. Appl. Earth Obs. Geoinf.* **2012**, *18*, 564–572.
21. Skakun, S.; Kussul, N.; Shelestov, A.; Kussul, O. The use of satellite data for agriculture drought risk quantification in Ukraine. *Geomat. Nat. Haz. Risk* **2016**, *7*, 901–917.
22. Rembold, F.; Atzberger, C.; Savin, I.; Rojas, O. Using low resolution satellite imagery for yield prediction and yield anomaly detection. *Remote Sens.* **2013**, *5*, 1704–1733.
23. Rembold, F.; Meroni, M.; Rojas, O.; Atzberger, C.; Ham, F.; Fillol, E. *Chapter 14. Agricultural Drought Monitoring Using Space-Derived Vegetation and Biophysical Products: A Global Perspective*; CRC Press: Boca Raton, FL, USA, 2015; pp. 349–365.
24. Kogan, F.N. Global drought watch from space. *Bull. Am. Meteor. Soc.* **1997**, *78*, 621–636.
25. Kogan, F.N. Droughts of the late 1980s in the United States as derived from NOAA polar-orbiting satellite data. *Bull. Am. Meteor. Soc.* **1995**, *76*, 655–668.
26. Zhang, A.; Jia, G. Monitoring meteorological drought in semiarid regions using multi-sensor microwave remote sensing data. *Remote Sens. Environ.* **2013**, *134*, 12–23.
27. Gebrehiwot, T.; van der Veen, A.; Maathuis, B. Spatial and temporal assessment of drought in the northern highlands of Ethiopia. *Int. J. Appl. Earth Obs. Geoinf.* **2011**, *13*, 309–321.
28. Singh, R.P.; Roy, S.; Kogan, F. Vegetation and temperature condition indices from NOAA AVHRR data for drought monitoring over India. *Int. J. Remote Sens.* **2003**, *24*, 4393–4402.
29. Seiler, R.; Kogan, F.; Sullivan, J. AVHRR-based vegetation and temperature condition indices for drought detection in Argentina. *Adv. Space Res.* **1998**, *21*, 481–484.
30. Unganai, L.S.; Kogan, F.N. Drought Monitoring and Corn Yield Estimation in Southern Africa from AVHRR Data. *Remote Sens. Environ.* **1998**, *63*, 219–232.
31. Sandholt, I.; Rasmussen, K.; Andersen, J. A simple interpretation of the surface temperature/vegetation index space for assessment of surface moisture status. *Remote Sens. Environ.* **2002**, *79*, 213–224.
32. Wang, P.X.; Li, X.W.; Gong, J.Y.; Song, C. Vegetation temperature condition index and its application for drought monitoring. In *Proceeding of the IEEE 2001 International Geoscience and Remote Sensing Symposium, IGARSS '01, Sydney, NSW, Australia, 9–13 July 2001*; pp. 141–143.
33. Wan, Z.; Wang, P.; Li, X. Using MODIS land surface temperature and normalized difference vegetation index products for monitoring drought in the southern Great Plains, USA. *Int. J. Remote Sens.* **2004**, *25*, 61–72.
34. Vicente-Serrano, S.M. Evaluating the impact of drought using remote sensing in a mediterranean, semi-arid region. *Nat. Hazards* **2007**, *40*, 173–208.
35. Zhang, F.; Zhang, L.W.; Wang, X.Z.; Hung, J.F. Detecting agro-droughts in southwest of China using MODIS satellite data. *J. Integr. Agric.* **2013**, *12*, 159–168.
36. Du, L.; Tian, Q.; Yu, T.; Meng, Q.; Jancso, T.; Udvardy, P.; Huang, Y. A comprehensive drought monitoring method integrating MODIS and TRMM data. *Int. J. Appl. Earth Obs. Geoinf.* **2013**, *23*, 245–253.
37. Mu, Q.; Zhao, M.; Kimball, J.S.; McDowell, N.G.; Running, S.W. A remotely sensed global terrestrial drought severity index. *Bull. Am. Meteor. Soc.* **2013**, *94*, 83–98.
38. Enenkel, M.; Steiner, C.; Mistelbauer, T.; Dorigo, W.; Wagner, W.; See, L.; Atzberger, C.; Schneider, S.; Rogenhofer, E. A combined satellite-derived drought indicator to support humanitarian aid organizations. *Remote Sens.* **2016**, *8*, 340.
39. Kogan, F.N. Remote sensing of weather impacts on vegetation in non-homogeneous areas. *Int. J. Remote Sens.* **1990**, *11*, 1405–1419.
40. Hird, J.N.; McDermid, G.J. Noise reduction of NDVI time series: An empirical comparison of selected techniques. *Remote Sens. Environ.* **2009**, *113*, 248–258.
41. Klisch, A.; Atzberger, C. Operational drought monitoring in Kenya using MODIS NDVI time series. *Remote Sens.* **2016**, *8*, 267.
42. Julien, Y.; Sobrino, J.A. Comparison of cloud-reconstruction methods for time series of composite NDVI data. *Remote Sens. Environ.* **2010**, *114*, 618–625.

43. Atkinson, P.M.; Jegathan, C.; Dash, J.; Atzberger, C. Inter-comparison of four models for smoothing satellite sensor time-series data to estimate vegetation phenology. *Remote Sens. Environ.* **2012**, *123*, 400–417.
44. Mishra, A.K.; Ines, A.V.; Das, N.N.; Khedun, C.P.; Singh, V.P.; Sivakumar, B.; Hansen, J.W. Anatomy of a local-scale drought: Application of assimilated remote sensing products, crop model, and statistical methods to an agricultural drought study. *J. Hydrol.* **2015**, *526*, 15–29.
45. Wu, J.; Zhou, L.; Zhang, J.; Liu, M.; Zhao, L.; Zhao, F. Analysis of relationships among vegetation condition indices and multiple-time scale SPI of grassland in growing season. In Proceedings of the 2010 18th International Conference on Geoinformatics, Beijing, China, 18–20 June 2010; pp. 1–6.
46. Quiring, S.M.; Ganesh, S. Evaluating the utility of the Vegetation Condition Index (VCI) for monitoring meteorological drought in Texas. *Agric. For. Meteorol.* **2010**, *150*, 330–339.
47. Ji, L.; Peters, A.J. Assessing vegetation response to drought in the northern Great Plains using vegetation and drought indices. *Remote Sens. Environ.* **2003**, *87*, 85–98.
48. Hijmans, R.J.; Cameron, S.E.; Parra, J.L.; Jones, P.G.; Jarvis, A. Very high resolution interpolated climate surfaces for global land areas. *Int. J. Climatol.* **2005**, *25*, 1965–1978.
49. Xiong, X.; Chiang, K.; Sun, J.; Barnes, W.; Guenther, B.; Salomonson, V. NASA EOS Terra and Aqua MODIS on-orbit performance. *Adv. Space Res.* **2009**, *43*, 413–422.
50. Huete, A.; Didan, K.; Miura, T.; Rodriguez, E.; Gao, X.; Ferreira, L. Overview of the radiometric and biophysical performance of the MODIS vegetation indices. *Remote Sens. Environ.* **2002**, *83*, 195–213.
51. Didan, K. MOD13Q1 MODIS/Terra Vegetation Indices 16-Day L3 Global 250 m SIN Grid V006. Technical Report, NASA EOSDIS Land Processes DAAC, 2015. Available online: <http://dx.doi.org/10.5067/MODIS/MOD13Q1.006> (accessed on 20 June 2016).
52. Miura, T.; Yoshioka, H.; Fujiwara, K.; Yamamoto, H. Inter-comparison of ASTER and MODIS surface reflectance and vegetation index products for synergistic applications to natural resource monitoring. *Sensors* **2008**, *8*, 2480–2499.
53. Fritz, S.; Bartholome, E.; Belward, A.; Hartley, A.; Stibig, H.J.; Eva, H.; Mayaux, P.; Bartalev, S.; Latifovic, R.; Kolmert, S.; et al. Harmonisation, Mosaicing and Production of the Global Land Cover 2000 database. Technical report, Joint Research Center, EC, 2003. Available online: <http://publications.jrc.ec.europa.eu/repository/handle/JRC26168> (accessed on 20 June 2016).
54. Bontemps, S.; Defournay, P.; Van Bogaert, E.; Arino, O.; Kalogirou, V.; Perez, J. GLOBCOVER 2009: Products Description and Validation Report. Technical Report, Université Catholique de Louvain (UCL) & European Space Agency (esa), 2011. Available online: http://due.esrin.esa.int/files/GLOBCOVER2009_Validation_Report_2.2.pdf (accessed on 20 June 2016).
55. Friedl, M.A.; Sulla-Menashe, D.; Tan, B.; Schneider, A.; Ramankutty, N.; Sibley, A.; Huang, X. MODIS Collection 5 global land cover: Algorithm refinements and characterization of new datasets. *Remote Sens. Environ.* **2010**, *114*, 168–182.
56. R Core Team. *R: A Language and Environment for Statistical Computing*; R Foundation for Statistical Computing: Vienna, Austria, 2016.
57. Hijmans, R.J. *Raster: Geographic Data Analysis and Modeling*, r Package Version 2.5-2 ed., 2015. Available online: <https://CRAN.R-project.org/package=raster> (accessed on 20 June 2016).
58. Dwyer, J.; Schmidt, G. The MODIS Reprojection Tool. In *Earth Science Satellite Remote Sensing*; Qu, J., Gao, W., Kafatos, M., Murphy, R., Salomonson, V., Eds.; Springer: Berlin, Germany, 2006; pp. 162–177.
59. Cleveland, W.S. LOWESS: A program for smoothing scatterplots by robust locally weighted regression. *Am. Stat.* **1981**, *35*, doi:10.2307/2683591.
60. Moreno, A.; García-Haro, F.J.; Martínez, B.; Gilabert, M.A. Noise reduction and gap filling of fapar time series using an adapted local regression filter. *Remote Sens.* **2014**, *6*, 8238–8260.
61. INE. *VII Censo Nacional Agropecuario y Forestal*; Instituto Nacional de Estadística (INE): Santiago, Chile, 2007.
62. Kogan, F.; Gitelson, A.A.; Zakarin, E.; Spivak, L.; Lebed, L. AVHRR-based spectral vegetation index for quantitative assessment of vegetation state and productivity: Calibration and validation. *Photogramm. Eng. Remote Sens.* **2003**, *69*, 899–906.
63. Beguería, S.; Vicente-Serrano, S.M. *SPEI: Calculation of the Standardised Precipitation-Evapotranspiration Index*, r Package Version 1.6 ed., 2013. Available online: <http://CRAN.R-project.org/package=SPEI> (accessed on 20 June 2016).

64. Bhuiyan, C.; Singh, R.; Kogan, F. Monitoring drought dynamics in the Aravalli region (India) using different indices based on ground and remote sensing data. *Int. J. Appl. Earth Obs. Geoinf.* **2006**, *8*, 289–302.
65. Bajgiran, P.R.; Darvishsefat, A.A.; Khalili, A.; Makhdoum, M.F. Using AVHRR-based vegetation indices for drought monitoring in the Northwest of Iran. *J. Arid. Environ.* **2008**, *72*, 1086–1096.
66. Mu, Q.; Heinsch, F.A.; Zhao, M.; Running, S.W. Development of a global evapotranspiration algorithm based on MODIS and global meteorology data. *Remote. Sens. Environ.* **2007**, *111*, 519–536.
67. Seiler, R.; Kogan, F.; Wei, G.; Vinocur, M. Seasonal and interannual responses of the vegetation and production of crops in Cordoba—Argentina assessed by AVHRR derived vegetation indices. *Adv. Space Res.* **2007**, *39*, 88–94.



© 2016 by the authors; licensee MDPI, Basel, Switzerland. This article is an open access article distributed under the terms and conditions of the Creative Commons Attribution (CC-BY) license (<http://creativecommons.org/licenses/by/4.0/>).